NTNU

Norwegian University of
Science and Technology

Vibrations from Magnetic Forces in Hydropower Generators

Jules Pascal

Master of Science in Electric Power Engineering
Submission date: June 2016
Supervisor: Arne Nysveen, ELKRAFT
Co-supervisor: Mostafa Valavi, ELKRAFT

Norwegian University of Science and Technology
Department of Electric Power Engineering

Abstract

Electrical machines using a fractional slot winding can be subject to low modes of vibration, which can produce noise and stator deformation. The design of a machine has an influence on the amplitude of these deformations, and it would be interesting to know how the design affects this amplitude. For this work, two different models of hydro-power generators have been developed on a Finite Element Analysis software. The results of the simulations for the machines under different loads have been exploited later on using a numerical computing environment and compared to withdraw conclusions about the effect of the design of a machine on low modes of vibration. The results showed that the slot width and the type of load have an influence on the amplitude of both lowest mode of vibration and zeroth mode. Now the effect of the slot width is certain, further work would be to investigate more on one of the machines to have a more precise idea of how evolves the amplitude of the zeroth and lowest mode for different slot widths.

NORGES TEKNISK-NATURVITENSKAPELIGE UNIVERSITET

NTNU

M A S T E R O P P G A V E

Kandidatens navn : Jules Pascal

Fag : **ELKRAFTTEKNIKK**

Oppgavens tittel (norsk) : Vibrasjoner fra magnetiske krefter i vannkraftgeneratorer

Oppgavens tittel (engelsk) : Vibrations from magnetic forces in hydropower generators

Oppgavens tekst:
In rotating electrical machines with radial air gap flux, there are large radial magnetic forces between the stator and rotor. They are normally balanced such that there is no net force on the rotor. Flux density waves in the airgap, and consequently radial force waves, are functions of both time and space. These rotating radial forces act on the stator and create vibration.

Radial magnetic forces are among the main sources for the vibration in the electrical machines. These forces, produced by the flux density waves, cause vibration and noise. In this project, the magnetic forces and vibration will be investigated in hydro generators. Two hydrogenerators have to be studied to investigate the effects of pole and slot combinations. The study uses FEM software for accurate calculation of the magnetic flux density.

More specifically the work shall focus on:

- Establish FEM models to calculate the magnetic field distribution during different operation conditions. The iron non-linearity and rotation should be included. Both magnetostatic and time-stepping analysis have to be carried out.
- Use Maxwell stress tensor to calculate the radial force density time and space distribution
- Analyse the force waves to predict the vibration characteristics
- Investigate the influences of pole and slot combinations and slot harmonics
- Study the lowest non-zero mode of vibration and zeroth-order radial forces

Further details of the work are to be discussed with the supervisors during the project period.

Acknowledgements

I want to sincerely thank my supervisor Arne Nysveen for offering me this subject and for his advices during the whole study. Also I am thanking ABB for providing such interesting thesis subjects to the university.
I am very thankful to Mostafa Valavi for his help and the interest he had for this work.
I also want to thank the NTNU committees, especially InterKom, and all the people I met here for making this year even better.
Finally, I want to express my gratitude to my parents for making this whole year possible.

Contents

List of Figures

1 Introduction

Electrical generators are the core of every kind of thermal power plant, wind turbines, hydroelectric dams, and more recently, wave power technologies. Each of them needs a generator with specific characteristics, including rotational speed. For example, thermal power plants will require high speed rotating machines, unlike hydroelectric dams and wind turbines, of which rotational speed is slower. As shown in (1), a slow machine requires a higher number of poles for the induced voltage to keep the required frequency, which is 50Hz for the grid.

$$n = \frac{2\pi f}{p} \tag{1}$$

n is the rotational speed of the machine(rad/s)
f is the frequency of the induced voltage(Hz)
p is the number of pair of poles

Also, a high number of poles means that the choices of number of slots are limited. Indeed, if the number of poles is high, increasing q, the number of slot per pole per phase, will significantly increase the number of slots as it can be seen in(2).

$$N_s = 2pmq \tag{2}$$

N_s is the number of slots
m is the number of phases of the machine
p is the number pair of poles
q is the number of slot per pole per phase

A fractional number of slots per pole allows more possibilities for the choice of number of slots.

Fractional slot winding machine means that q, the number of slot per pole per phase, is not an integer as it usually is for machines with a smaller number of poles. Additionaly to the flexibility it gives to the number of slots, this solution makes the stator manufacturing easier and cheaper[1].

For instance, in the case of a 40 poles three phase machine: An integer slot winding requires to have 120 slots for q=1, 240 slots for q=2 or higher multiples of 120 for a higher q. But it might be beneficial for the machine to have a number of slots between 120 and 240. Then it is necessary to make a fractional slot winding stator. Because it is a three-phase machine, the number of slots must be a multiple of 3. Then, a possible choice would be 180 slots, and the number of slot per pole per phase $q = 1, 5$.

The second main benefit of a fractional slot winding is the reduction of the harmonic content of the back emf voltage, as [2] highlights it comparing the total harmonic distortion(THD) of both distributed and fractional slot winding machines. Besides the reduction of the harmonic content and the enlargement of the number of slots choice, a fractional slot winding also reduces the cogging torque of a machine[2].

The cogging torque is produced by the poles trying to align with the maximum amount of stator steel[3]. It actually tries to maximize the flux crossing from rotor to stator.

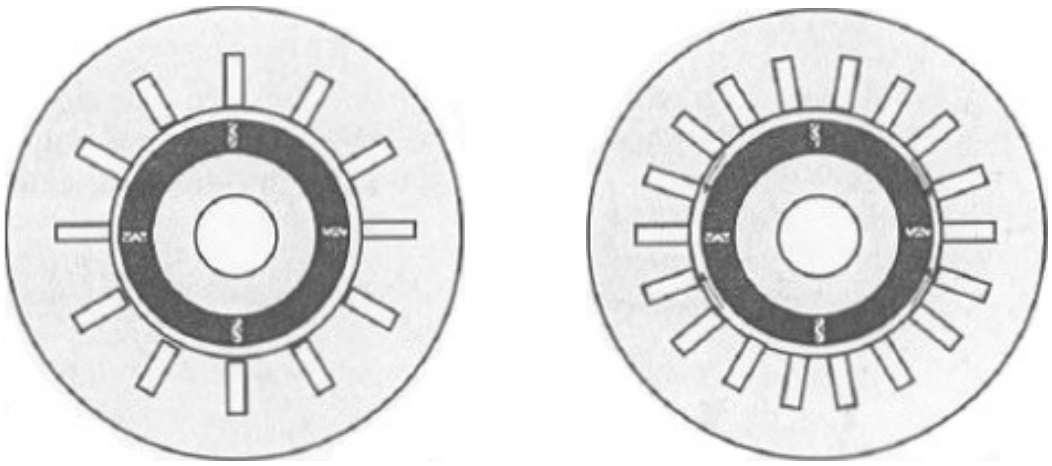

(a) q=1 (b) q=1.5

Figure 1: Machines with different number of slots per pole per phase[3]

Figure 1a highlights how every pole is in the same position relatively to the stator teeth. Therefore, the total cogging torque is equal to the sum of those forces produced by each magnet. On the other hand, the adjacent magnets of the machine Figure 1b are aligned differently with the stator teeth, which means cogging torque produced by adjacent magnets are out of phase with each other. This fact is shown in Figure 1b by the arrows indicating the cogging torque direction produced by each magnet. In the ideal case, the cogging torque produced by each magnet in cancelled by a net equal and opposite directed torque produced by the other magnets. In reality, this cancellation is never perfect, but a substantial reduction of the cogging torque is possible[3]. This type of winding makes an important difference in the distribution of the flux in the air gap of the machine. Indeed, when all the poles of an integer slot winding machine would always face the same number of teeth at the same instant, it would not be the case for the poles of a fractional slot winding machine.

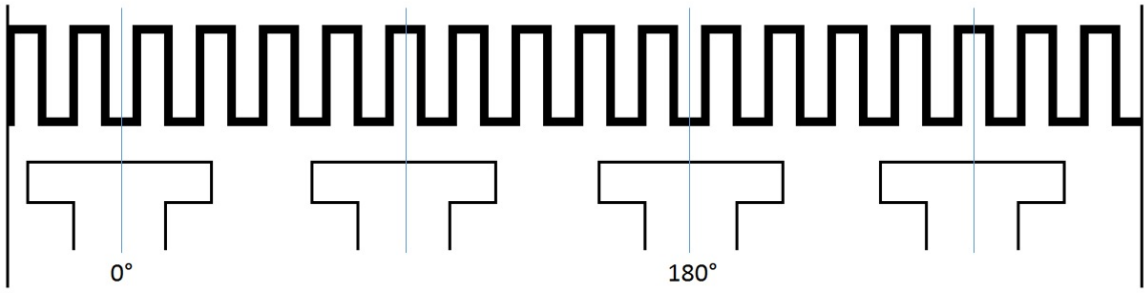

Figure 2: Poles facing slots

In Figure 2, the 4 poles of this 18 slots machine are not facing their respective slots the same way. Then, while the flux density in the air gap of each pole should be the same, there will be a slight difference from one pole to another. Thus, the radial radial flux density in the air-gap at 0°(electrical) will be different from the one at 180°(electrical). In this particular case, the middle of the first pole is facing a tooth, meanwhile the middle of the second pole, which is located at 90°(mechanical) from the first pole, is facing a slot. This means the first stator part is facing the highest maximum radial flux density a stator part can be facing, while at 90°(mechanical) apart from the first rotor pole, the second stator part faces the lowest maximum radial flux density it could be facing. On the flux density distribution, this creates a harmonic, whose order is lower than the order of the main harmonic created by the poles. Those harmonics are called sub-harmonics and have to be considered because of the low mode of vibration they can produce. A mode of vibration is not necessarily a threat for the machine if its order is higher or equal to two because the net force is symmetrical. The higher order the better, but this will be discussed in the part about vibrations.
Even though there is a symmetry in the net force, the forces can be quite large, which could result in a significant deformation of the stator. This drawback is specific to the fractional slot winding as there can't be sub-harmonics in the flux density distribution of an integer slot winding machine, because the greater common divisor(GCD) of the number of slots and the number of poles pairs will be the number of poles pairs, which makes the main harmonic the one that has the lowest order.

Another vibration mode that will be investigated in this paper is the mode of order 0. Contrarily to those mentioned before, the zeroth mode is not space related, but time related. What is meant is that the mean value of the radial forces applied to the stator is different from one moment to another. Even though the dominant mode of vibration is the lowest non-zero mode and the effects of the zeroth mode are not always considerable, it is worth to investigate its characteristics[4].

A machine needs to be studied in order to be aware of the amplitude of the sub-

harmonic and the mode of vibration because of the consequences high deformations can have on the stator. Because this deformation is produced by electromagnetic forces, it is necessary to evaluate the magnetic flux density in the air-gap. This can be done analytically or with a finite element method(FEM) software. For a better accuracy, the second method will be used.

1.1 Problem description

Radial magnetic forces are among the main sources for the vibration in electrical machines. These forces, produced by the flux density waves, act on the stator bore and cause vibrations and noise. In this project, the magnetic forces and vibration will be investigated in the hydro generators. The focus is on the fractional-slot windings.

As the first step, magnetic field distribution shall be computed in the generator using time-stepping finite-element analysis. Then, employing Maxwell stress tensor, time and space distribution of the radial force density will be calculated. Radial force density will be analysed to investigate vibration characteristics. Both lowest non-zero mode of vibration and zeroth radial forces shall be studied. Influence of loading and pole/slot combinations on the magnetic forces and vibration is planned to be addressed. The simulation results should be used to discuss the important factors in the vibration characteristics of the hydro generators.

1.2 Background and aim

To run those simulations, it is needed to develop a model of the studied generator on a finite-element analysis software. In the project foregoing this thesis has been created a customizable model that would make the development of a machine design easier as it wouldn't be necessary to create it from the beginning. Thus, it will be possible to run similar simulations for two different hydro power generators and then draw conclusions about the influence of the design of a machine on the field distribution and the flux density waves.

The aim of this thesis is to develop the model of a second hydro power generator on Ansys Maxwell and run the same simulations as the first machine. Then a Matlab script that will exploit the results from those simulations should be developed to evaluate the forces on the stator.

2 Forces and Vibrations

Sources of noise in electrical machines can be mechanical, aero-dynamical, or electromagnetic. Mechanical noises usually come from the bearings, thus they exist for most of the machines but are not the main source of noise, especially in the case of low rotational speed machines[5]. Also they can be reduced with the quality of the bearings and the oil, or suppressed with magnetic bearings technologies. Aero-dynamical noises are caused by rotating part creating air turbulence. They mainly depend on the design of the machine's rotor and are not a source of concern in low-speed machines either. Electromagnetic noises are even more important to consider in low-speed machines as the frequency of those noises can be close to the natural frequency of the machine's structure, which would dramatically amplify the vibration and the noise[6].

2.1 Origin of the vibrations

2.1.1 Flux density in the air gap

The currents flowing in the conductors of the machine create a magnetic field in the air gap. This magnetic field acts both on the stator and the rotor iron, and two kinds of forces appear in the rotating machine:

- Tangential forces, creating torque and rotor rotation
- Radial forces, which tend to attract stator and rotor

While the rotor vibrations from magnetic forces are not taken into account because of the rotor rigidity, those from the stator have to be considered as the magnetic forces can deform it and create vibrations. Also, the radial forces increasing with the surface the flux is going through, the stator is more likely to be deformed than the rotor[5]. The flux density in the air gap contains a fundamental component and a lot of harmonics generated by[5]:

- Space harmonics, which affect the magneto motive force
- The variable reluctance caused by the variable length of the air gap
- The eventual eccentricity of the rotor, creating variable minimal value of the air gap thickness; due to radial forces, manufacturing, or ageing of the bearings
- The magnetic saturation of the steel sheets
- The current harmonics due to the power supply

If a machine has to be silent, those harmonics have to be as small as possible.

2.1.2 Radial magnetic forces

Radial magnetic forces are a significant source of vibrations in electrical machines and they can be evaluated with the radial and tangential components of the magnetic flux density in the air-gap, using the following formula[7]:

$$f_r = \frac{1}{2\mu_0}(B_r^2 - B_t^2) \tag{3}$$

Those 3 quantities depend on the angular position and the time. Although Br and Bt can be calculated for different points in the air-gap with a finite element analysis software, the radial magnetic force density in the air-gap is also expressed by the general formula:

$$f_r(\theta, t) = f_{r,max} \cos(m\theta - k\omega t) \tag{4}$$

θ is the angular mechanical position
t is the time
k is the time harmonic number
ω is the angular velocity
m is the mode number that will be discussed in section about the deformation modes

The radial forces can deform the stator, and the amplitude of the deformation is inversely proportional to m^4[5]. Machines having a low mode number are thus more likely to have important vibrations.

2.2 Deformation mode

The mode number corresponds to the number of forces acting on the stator. It is equal to the GCD of the number of slots and the number of poles, and is equal to the number of pole in integral slot winding machines. Nevertheless, it can be as low as 1 for fractional slot winding machines. The stator can have a different deformation mode, depending on the value of m[5][8].

- m=1 is a specific case where there is no symmetry in the net force of the machine. The strongest attraction force between rotor and stator is located at 180°(mechanical) from the weakest force. The rotor is then off center as shown Figure 3. This case is rare and usually caused by a rotor eccentricity rather than a fractional slot winding.

- m=2 is more common as the two strongest forces have a 180°(mechanical) phase-shift, which makes a symmetry in the net force. It might however be the source of important stator deformations. The amplitude of the deformation will be discussed later on, but the comparison between m=2 and m=4 in the Figure

4 already suggest that a greater mode number leads to a smaller amplitude of deformation.

- m=0 is different from the other modes as it is not space related but time related. A zero-mode number means that the average value of the magnetic forces on the stator is changing over time, which leads to a varying but symmetric pressure all along the stator as it is shown on Figure 5.

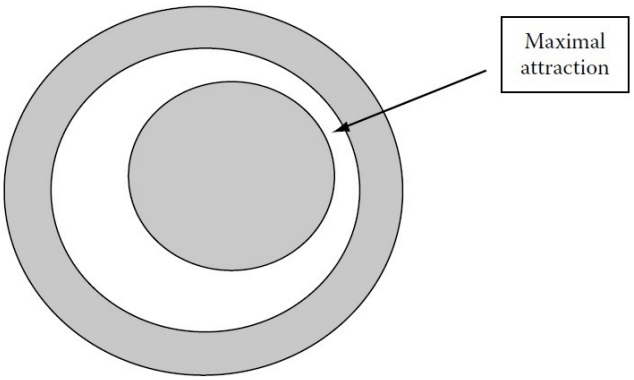

Figure 3: Rotor displacement for m=1 [5]

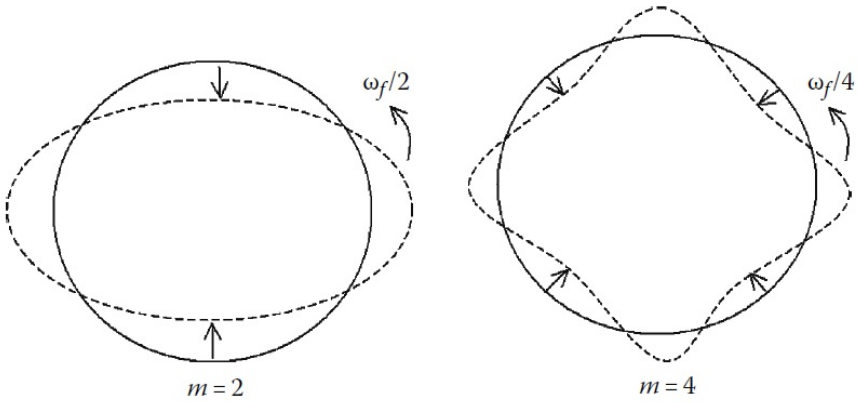

Figure 4: Stator deformation for m=2 and m=4 [5]

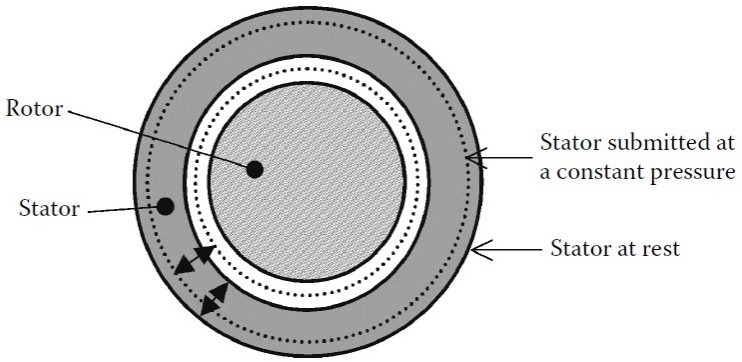

Figure 5: Rotor displacement for m=0 [5]

2.3 Amplitude of the static distortion and resonance frequencies

For a given value of amplitude of a force on the stator, the amplitude of the deformation, noted Y_{ms}, is defined by the following relationship:

$$Y_{ms} = \frac{12RR_y^3\hat{f}_{mM}}{ET_y^3(m^2-1)^2} \tag{5}$$

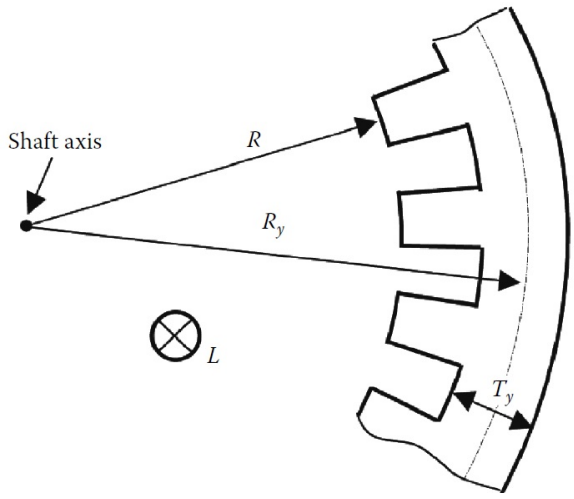

Figure 6: Notations for the stator frame [5]

The notations used in this relationship are the following:
R is the internal radius of the stator
R_y is the yoke average radius
T_y is the yoke radial thickness
L is the iron length
L_s is the distance between rotor shaft supports
d is the diameter
E is the elasticity coefficient or Young's modulus: $E = 2.1 \times 10^{11} N/m^2$ for iron

As can be seen in (6), the amplitude of the distortion increases greatly as m decreases , which makes a low mode number more dangerous for the stator structure. Practically, forces having a mode number higher than 8 are not considered[5]. It is worth mentioning that the amplitude of the distortion is proportional to the radius of the stator(6). Also, T_y is inversely proportional to the number of pole pairs, which makes the amplitude of the distortion proportional to the number of poles. Hence, it is important to consider those distortions in machines with a high number of poles as they usually have a relatively smaller yoke width.

The frequency of a force is also an important factor, influencing the amplitude of the vibration. Chances of having a force frequency close to the natural resonance frequency of the stator structure are higher if the force frequency is low. The natural resonance frequency of a structure is the one the structure keeps oscillating at after being hit. Consequently, if the frequency of a force variation is close to a resonance frequency, the system is more likely to produce noise and to vibrate more[5]. Thus, it is also a source of concern in electrical machines having a low deformation mode.

3 Finite element analysis

The aim of this project was to create the model of a machine on the FEM software Ansys Maxwell and to obtain the traces of the magnetic flux density in different cases of simulations. In a previous project has been developed a customizable model, allowing to model a machine quickly just by changing parameters such as the number of poles, slots, diameters, pole and slot width and more. Then it has been possible to reproduce the design of two machines and run the same simulations on those different generators.

The machines have the following characteristics:

Machine	**1**	**2**
Power	105MVA	320MVA
Number of poles	14	14
Number of slots	180	114
Length of the machine	1.8m	3.6m
Voltage(2 parallel circuits)	11kV	16.6kV
Total excitation(no load)	26125A	28470A
Total excitation(load)	57855A	62400A
Fp Inductive load	0.9	0.86
Speed	428.57 rpm	428.57 rpm

Appendix 2 provides more informations about the design specifications of the first machine. The documentation about the second machine should be asked to the supervisor of this thesis, Arne Nysveen.

3.1 Winding of the machines

Both machines have the same number of poles, but they have a different number of slots, which means their winding will be different.

In machine 1, their are 180 slots and 14 poles, hance $q = 4 + \frac{2}{7}[1]$. Then the winding is the following[9]:

Slot n°	1	2	3	4	5	6	7	8	9	10	11	12	13
Phase R	1	1	1	1	1								
Phase S										1	1	1	1
Phase T						-1	-1	-1	-1				

Slot n°	1	2	3	4	5	6	7	8	9	10	11	12	13	14	15	16	17	18	19	20
Layer 1	R	R	R	R	R	-T	-T	-T	-T	S	S	S	S	-R	-R	-R	-R	-R	T	T
Layer 2	R	-T	-T	-T	-T	S	S	S	S	-R	-R	-R	-R	-R	T	T	T	T	-S	-S

Slot n°	21	22	23	24	25	26	27	28	29	30	31	32	33	34	35	36	37	38	39	40
Layer 1	T	T	-S	-S	-S	-S	R	R	R	R	-T	-T	-T	-T	-T	S	S	S	S	-R
Layer 2	-S	-S	R	R	R	R	R	-T	-T	-T	-T	S	S	S	S	-R	-R	-R	-R	T

Slot n°	41	42	43	44	45	46	47	48	49	50	51	52	53	54	55	56	57	58	59	60
Layer 1	-R	-R	-R	T	T	T	T	T	-S	-S	-S	-S	R	R	R	R	-T	-T	-T	-T
Layer 2	T	T	T	T	-S	-S	-S	-S	R	R	R	R	-T	-T	-T	-T	-T	S	S	S

Slot n°	61	62	63	64	65	66	67	68	69	70	71	72	73	74	75	76	77	78	79	80
Layer 1	S	S	S	S	S	-R	-R	-R	-R	T	T	T	T	-S	-S	-S	-S	-S	R	R
Layer 2	S	-R	-R	-R	-R	T	T	T	T	-S	-S	-S	-S	-S	R	R	R	R	-T	-T

Slot n°	81	83	83	84	85	86	87	88	89	90
Layer 1	R	R	T	T	T	T	S	S	S	S
Layer 2	-T	-T	S	S	S	S	S	-R	-R	-R

Figure 7: Winding Machine 1

For one phase, it would need $7q$ to get to an integer number of slots, that is 30 slots. Thus, for three phases, 90 slots are necessary, which is the winding Figure 7. The machine having 180 slots in total, the scheme Figure 7 will repeat twice in the whole stator.

In machine 2, their are 114 slots and 14 poles, hance $q = 2 + \frac{5}{7}[1]$. Then the winding is the following[9]:

Slot n°	1	2	3	4	5	6	7	8	9	10	11	12	13	14	15	16	17
Phase R	-1	-1	-1							1	1						
Phase S				1	1	1						-1	-1	-1			
Phase T							-1	-1	-1						1	1	1

Slot n°	1	2	3	4	5	6	7	8	9	10	11	12	13	14	15	16	17	18	19	20
Layer 1	-R	-R	-R	S	S	S	-T	-T	-T	R	R	-S	-S	-S	T	T	T	-R	-R	S
Layer 2	-R	-R	-R	S	S	S	-T	-T	R	R	R	-S	-S	-S	T	T	T	-R	-R	S

Slot n°	21	22	23	24	25	26	27	28	29	30	31	32	33	34	35	36	37	38	39	40
Layer 1	S	S	-T	-T	-T	R	R	R	-S	-S	T	T	T	-R	-R	-R	S	S	-T	-T
Layer 2	S	S	-T	-T	-T	R	R	-S	-S	-S	T	T	T	-R	-R	-R	S	S	-T	-T

Slot n°	41	42	43	44	45	46	47	48	49	50	51	52	53	54	55	56	57
Layer 1	-T	R	R	R	-S	-S	-S	T	T	-R	-R	-R	S	S	S	-T	-T
Layer 2	-T	R	R	R	-S	-S	T	T	T	-R	-R	-R	S	S	S	-T	-T

Figure 8: Winding Machine 2

For the second machine, it would need $7q$ to get an integer number of slots for one phase as well, that is 19 slots. Thus, for three phases, 57 slots are necessary, which is the winding Figure 8. The machine having 114 slots in total, the scheme Figure 7 will also repeat twice in the whole stator.

3.2 Modeling

The first machine was the generator used to create the customizable model, while the second machine has been created from the first machine, changing the design in the parameters. Only the particular shape of the poles required changes out of the basic parameters of the machine. Then, rotor excitation has been set and the stator winding has been made as explained in the previous section. Figures 9 and 10 show the design of the machines and the flux lines from the rotor excitation.

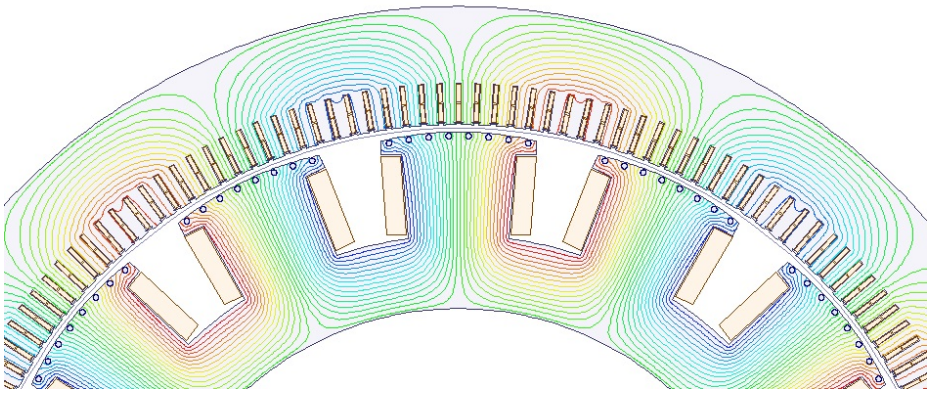

Figure 9: Flux lines machine 1 at initial position(no load) [10]

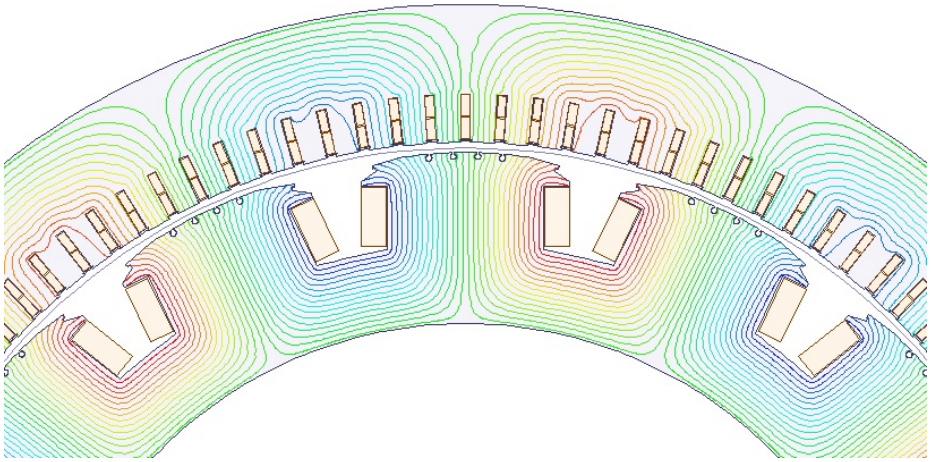

Figure 10: Flux lines machine 2 at initial position(no load) [10]

The mesh density has to be high enough for both machines because of some elements of the design such as sharp angles and the damper bars. Each meshing had an element maximum length of 5mm and 20000 elements maximum, for each stator and rotor, which makes 40000 elements maximum for each machine. Figures 11 and 12 show that it provides a mesh dense enough for the simulations.

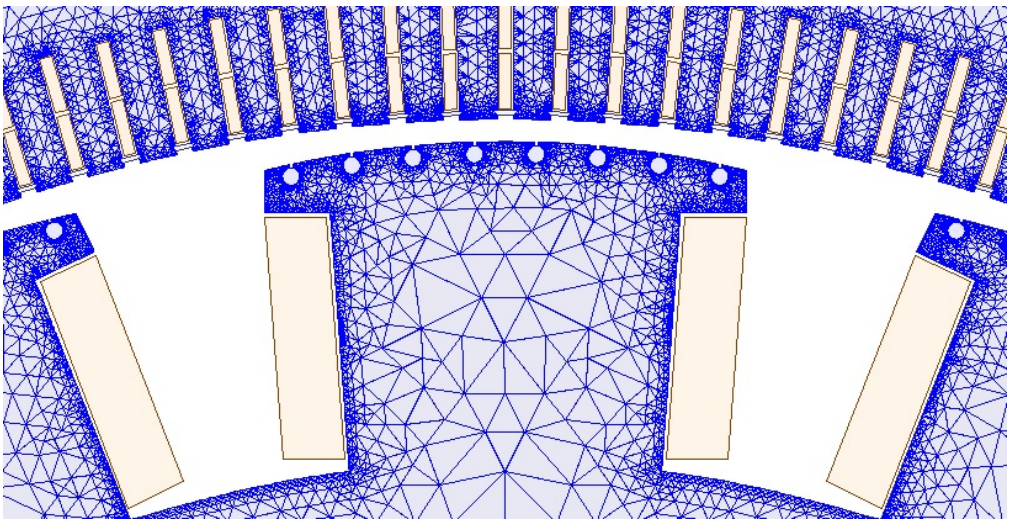

Figure 11: Meshing Machine 1 [10]

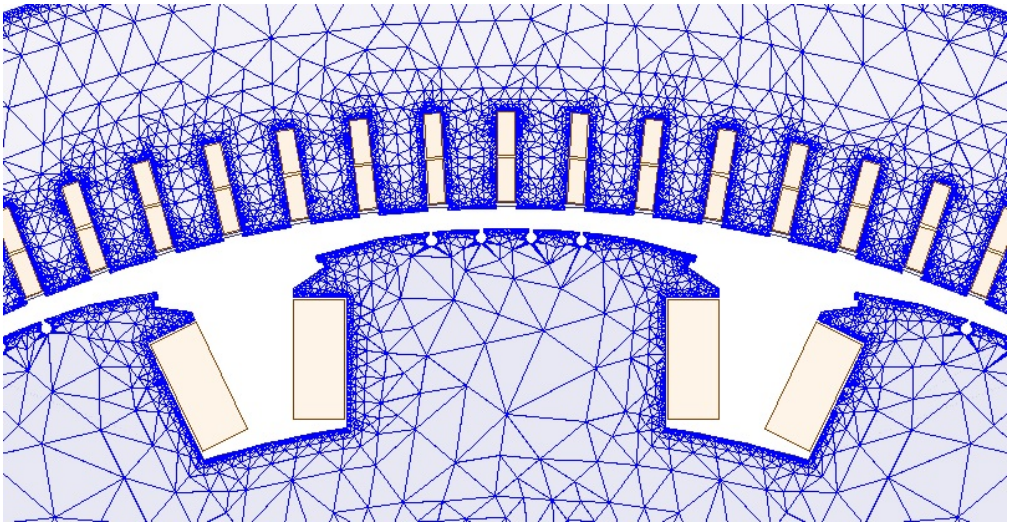

Figure 12: Meshing Machine 2 [10]

Last step of modelling was to assign the materials for the rotor and the stator of the machine. The laminated steel assigned to the stator was the M300-35A, and its proprieties are in the appendice 1 and in the B-H curve Figure 13a. The material that has been assigned to the rotor is the steel 1010 which was in the Maxwell library, to which were added 4 times the losses of the M300-35A. Figure 13b show the B-H curve of the steel 1010.

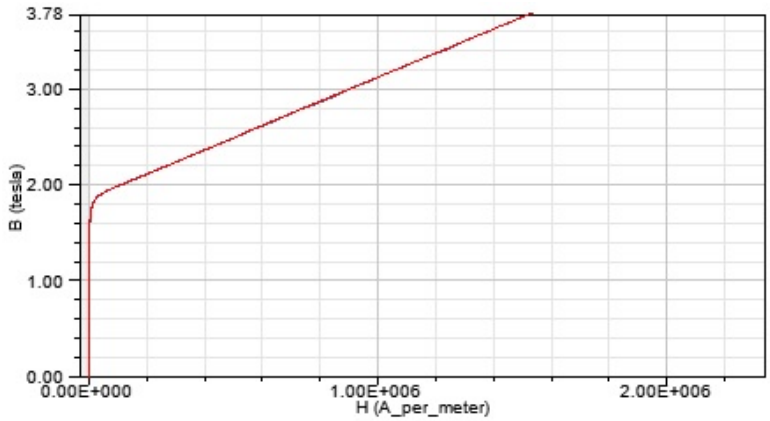

(a) B-H curve material M300-35

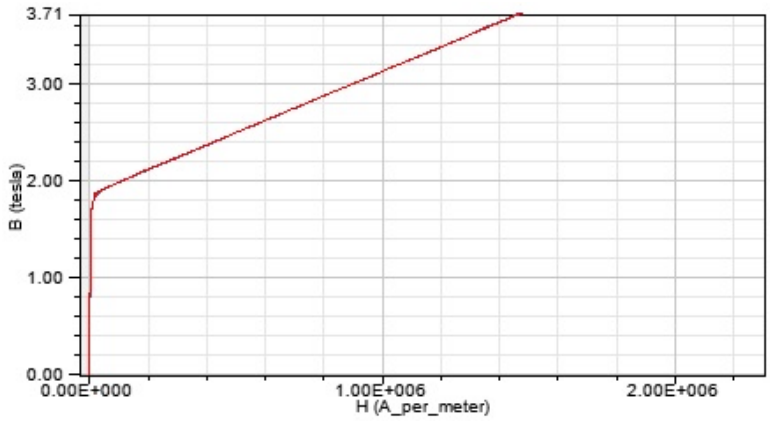

(b) B-H curve material steel 1010

Figure 13: B-H curves of the stator(a) and rotor(b) materials

Magnetostatic simulations have been run for both machines to make sure the models were correct. Once the models were validated, transient simulations started. The first time stepping simulation for both machines is at no load. Then, the same simulation has to be run with the external circuits shown Figure 14, 15(only for machine 2), 16 and 17 that are resistive, inductive and capacitive loads respectively.

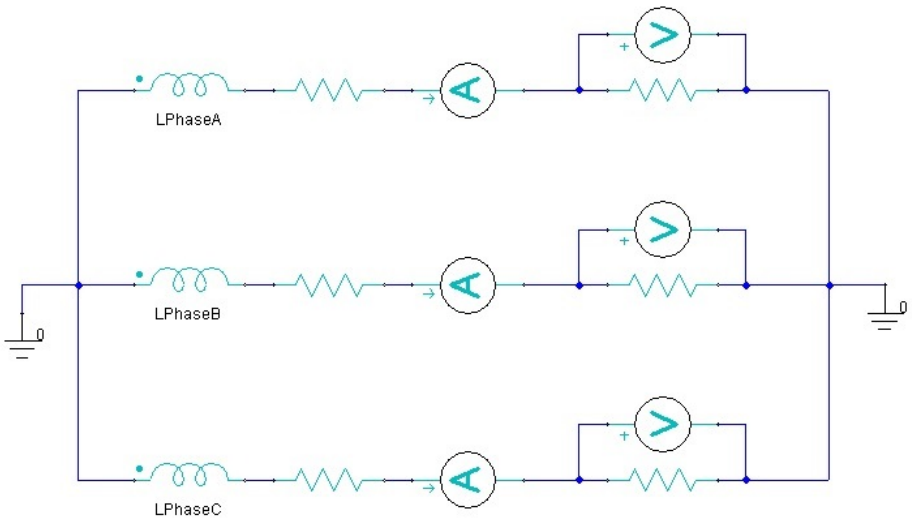

Figure 14: External circuit of the resistive load of each machine
Machine 1: $R_{line} = 0.002245\Omega$, $R_{load} = 5.5\Omega$,
Machine 2: $R_{line} = 0.00169\Omega$, $R_{load} = 3.55\Omega$

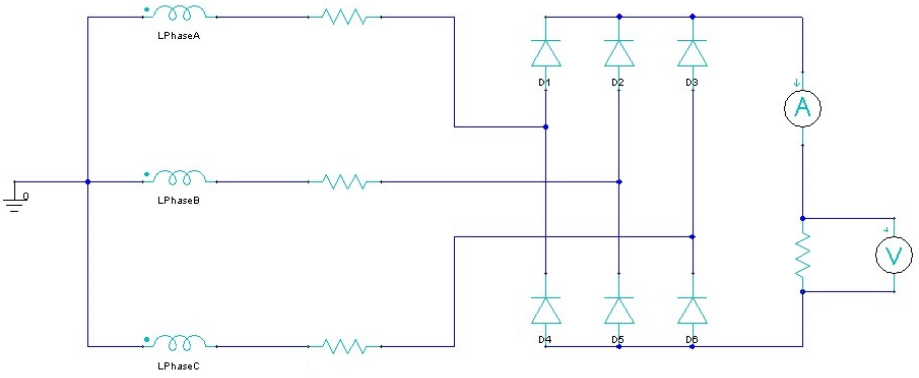

Figure 15: External circuit of the diode rectifier load for machine 2
$R_{line} = 0.00169\Omega$, $R_{load} = 3.8\Omega$

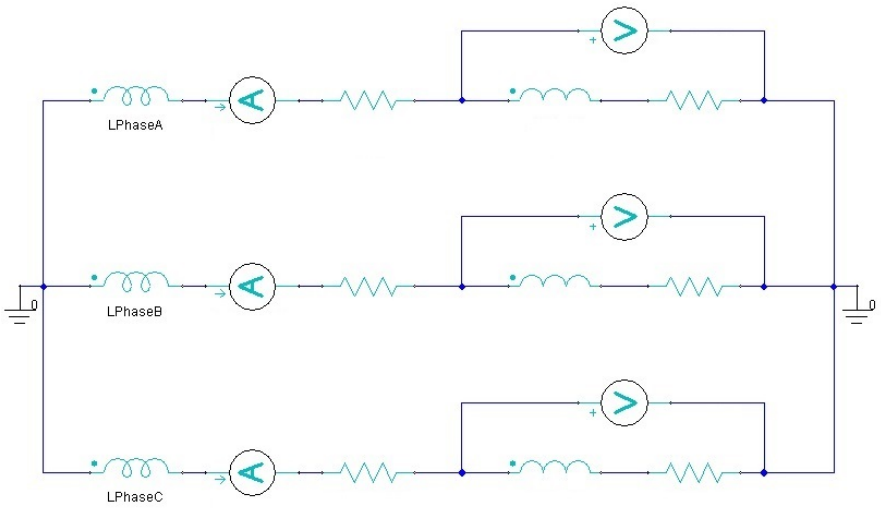

Figure 16: External circuit of the inductive load of each machine
Machine 1: $R_{line} = 0.002245\Omega$, $R_{load} = 4.135\Omega$, $L = 6.66mH$
Machine 2: $R_{line} = 0.00169\Omega$, $R_{load} = 2.2217\Omega$, $L = 4.1963mH$

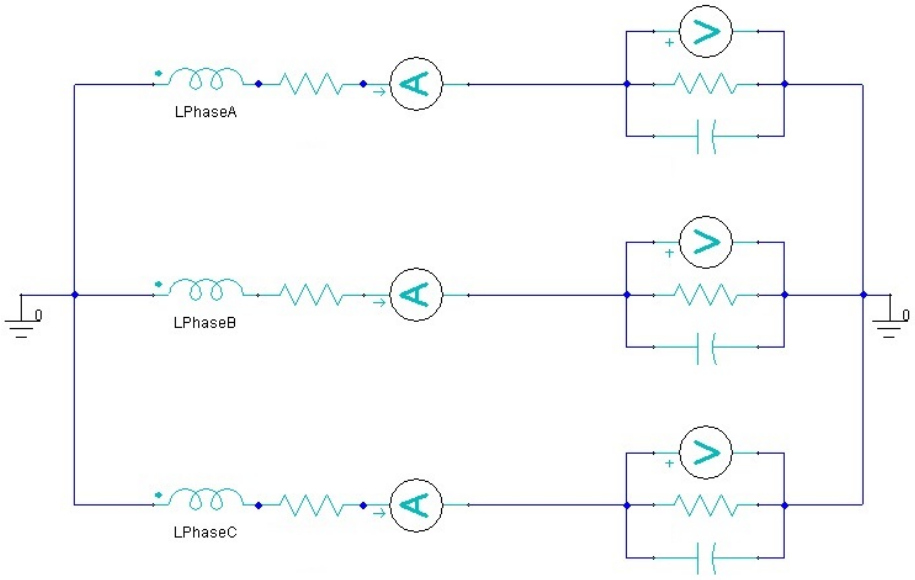

Figure 17: External circuit of the capacitive load of each machine
Machine 1: $R_{line} = 0.002245\Omega$, $R_{load} = 7.2\Omega$, $C = 213.458\mu F$
Machine 2: $R_{line} = 0.00169\Omega$, $R_{load} = 5.25\Omega$, $C = 359.43\mu F$

4 Results of the simulations

This part will discuss the results of the simulations for both machines in two cases.

- Case 1 is a machine without a load. The voltage will be considered first to ensure the models give results close to what is expected. Then the flux distribution and the radial forces should be studied.
- Case 2 is a machine with an inductive load, with a power factor equal to 0,9 for the first machine and 0,86 for the second. In this case, the current will be studied additionally to the voltage, flux density, and radial forces.

The same simulations have also been done with a resistive load and a capacitive load on both machines, and with a diode rectifier and a resistive load for the second machine, but the results given by the inductive load were more relevant. Therefore, this paper focuses on the no load and inductive load case, also the diode rectifier and resistive loads' zeroth-mode will be investigated.

4.1 No load case

The first step to validate the model in a transient solution type is to verify the voltage between two phases in a case with no load.

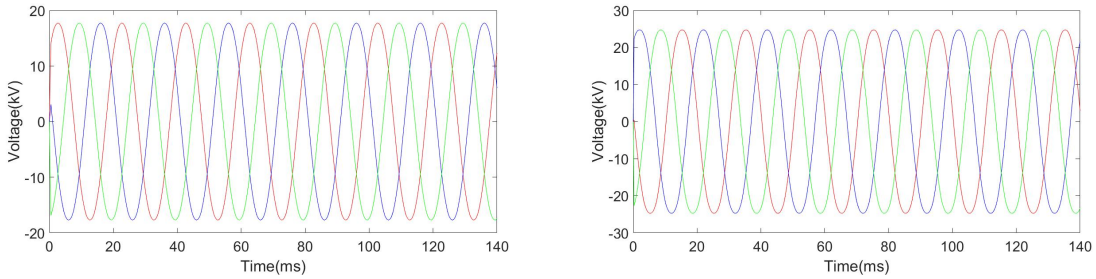

(a) Machine 1: $U = 20.65kV$ (b) Machine 2: $U = 31.75kV$

Figure 18: Voltages at no load

The voltage levels are close to what was expected, also the three phases are balanced. They are twice as high as the voltages from the documentations of the machines, but it is explained by the winding that is supposed to be 2 parallel circuits. On the simulation models, each machine only has one circuit. It is then normal to see the voltage doubled.

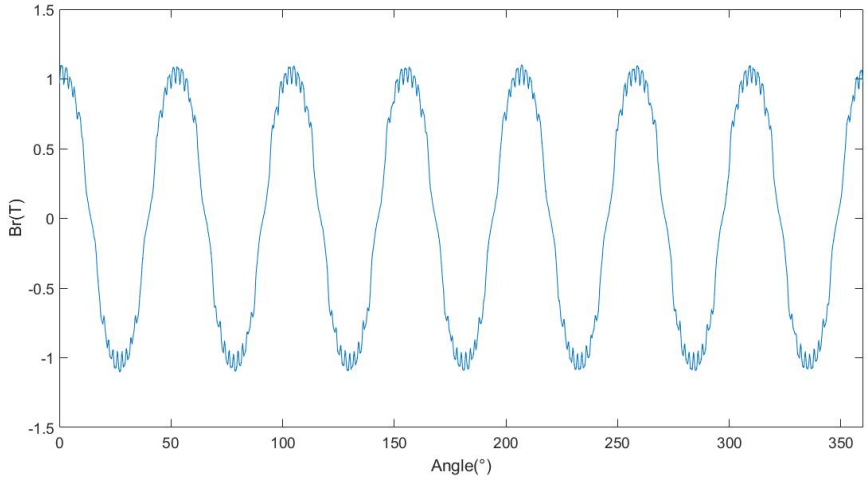

(a) Machine 1

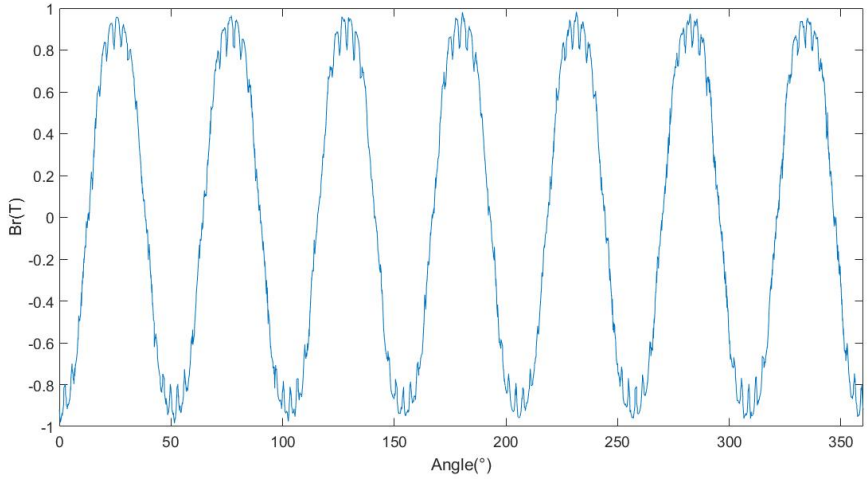

(b) Machine 2

Figure 19: Distribution of the radial flux density in the air-gap at one moment(when the voltage is the highest for one phase) (no load)

Figure 19a and 19b highlight the waveform from the poles when a phase has the highest voltage($t = 60.48ms$). The main wave corresponds to the poles of the machine, as it has 7 periods among 360°. It is also possible to count the number of slot that are physically above each pole to the number of "teeth" each pole's wave has. However, it is interesting to notice that no sub-harmonic is visible on the radial flux density distribution.

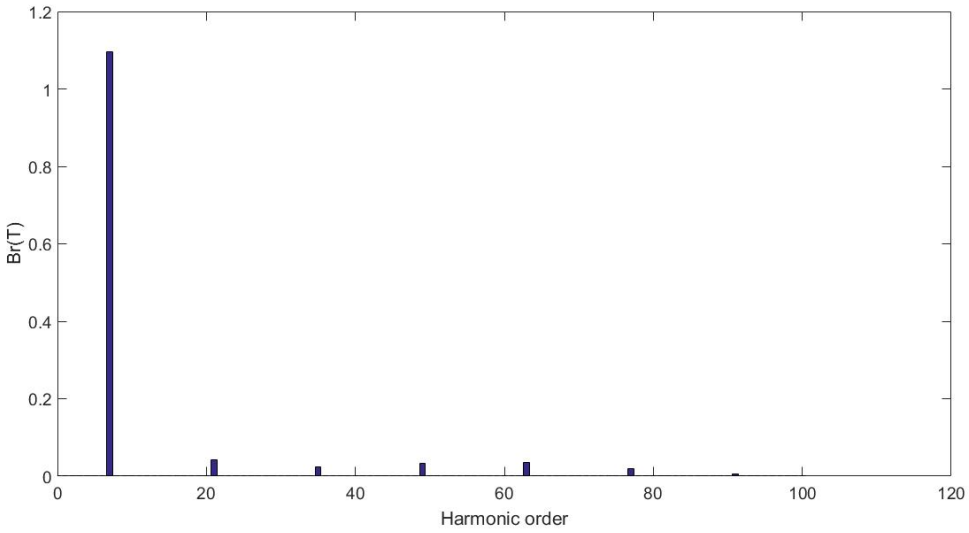

(a) Machine 1

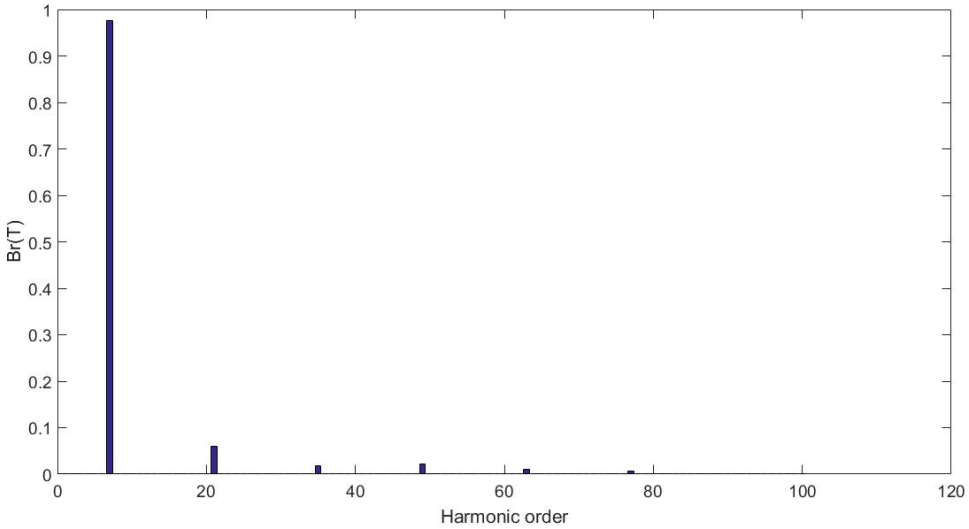

(b) Machine 2

Figure 20: Harmonic content of the radial flux density in the air-gap at one moment(when the voltage is the highest for one phase) (no load)

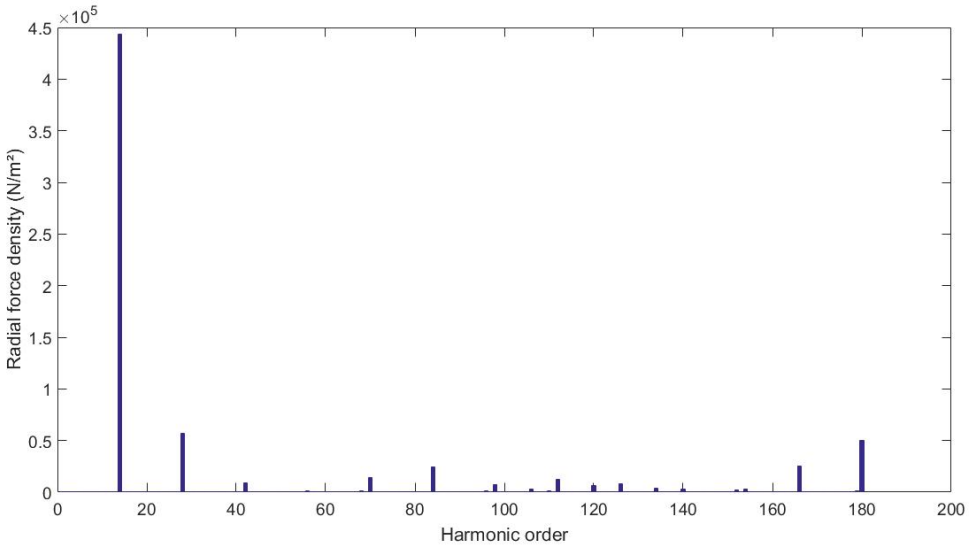

(a) Machine 1

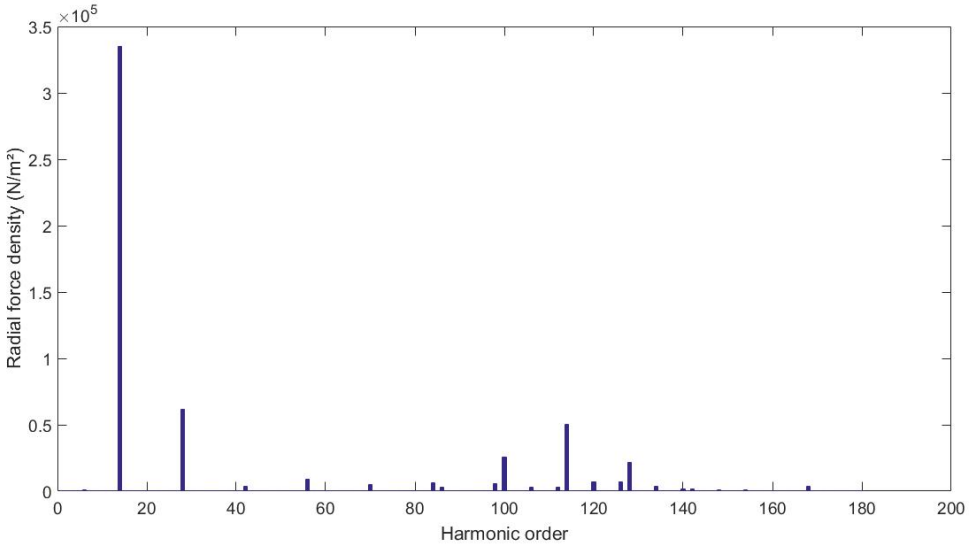

(b) Machine 2

Figure 21: Harmonic content of the radial force at one moment(when the voltage is the highest for one phase) (no load)

The harmonic content of both radial flux density and radial force Figures 20 and 21 show the harmonic of second order's amplitude is negligible. Therefore, it shouldn't be considered in this case. Figures 21a and 21b nonetheless allow to notice

the amplitude of the radial force created by the poles, and also by the slots. It is worth to notice that the poles and slots harmonics are quite large while the harmonic of second order isn't. Indeed, this can mean that the load increases the interaction between poles and slot that is supposed to be the main responsible for the existence of the harmonic of lowest order, as it is concluded in [11]. It can also be noted that the amplitude of the pole harmonic is larger in the first machine than in the second, but the amplitude of the slot harmonic is the same, despite the difference of slot width between the first and the second machine.

4.2 Inductive load case

In this part will be studied the results of the simulations ran on the same machines with an inductive load and a higher excitation in the rotor.

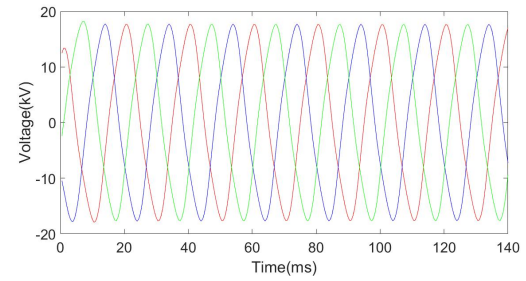

(a) Voltage Machine 1

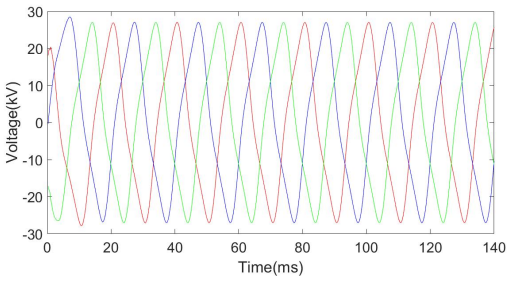

(b) Voltage Machine 2

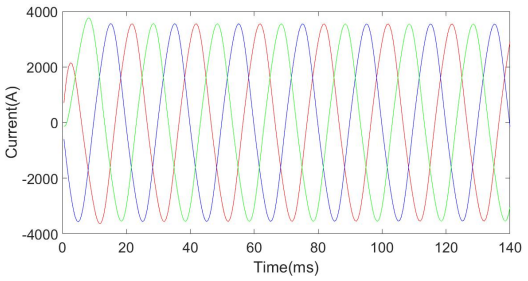

(c) Current Machine 1

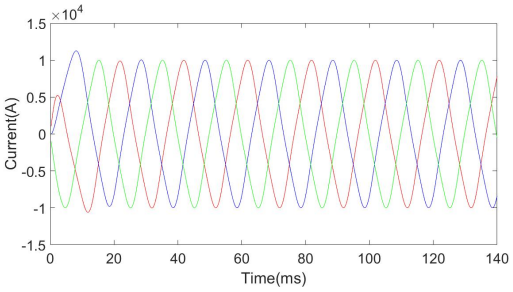

(d) Current Machine 2

Figure 22: Voltages and currents(RL)

The three-phases voltage and current seem to be almost purely sinusoidal, have correct levels and are balanced. The harmonic content of those voltages and currents confirm this first observation.

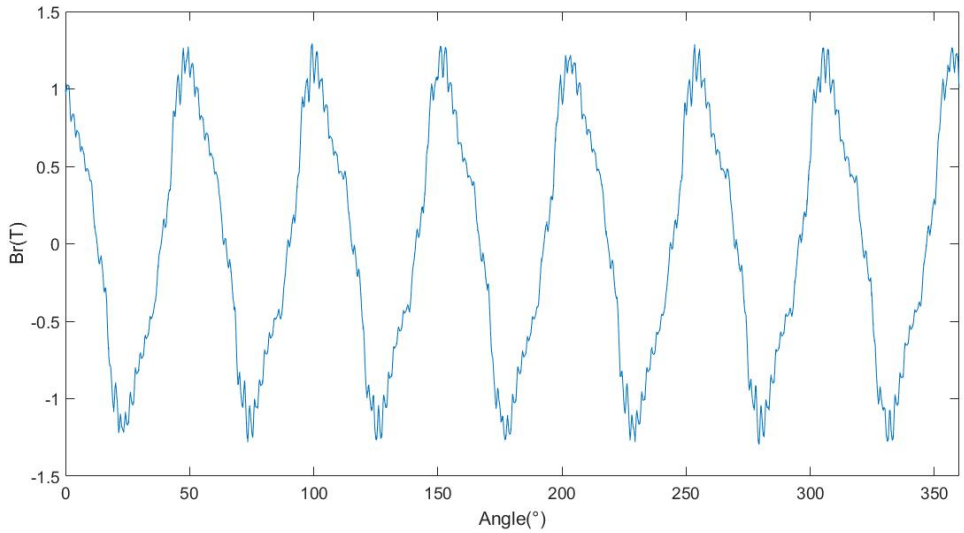

(a) Machine 1

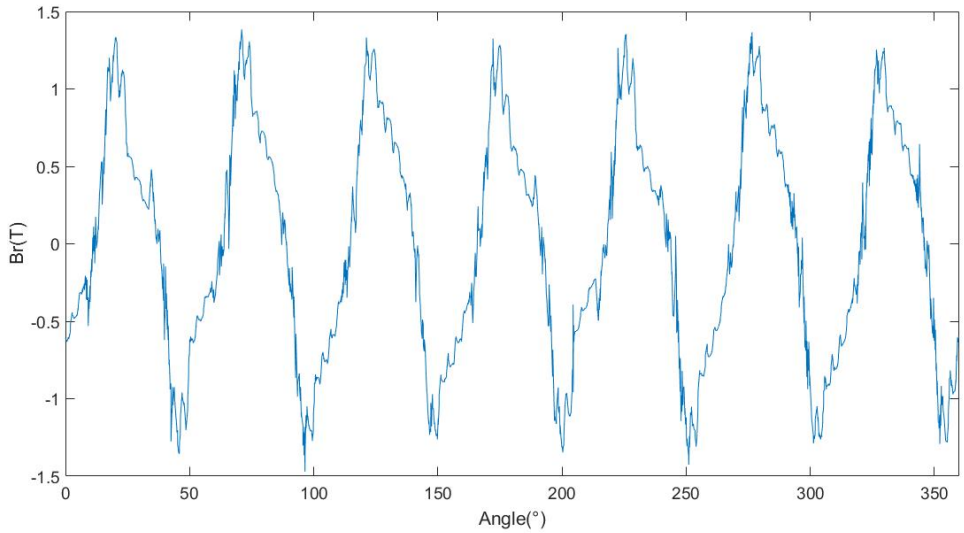

(b) Machine 2

Figure 23: Distribution of the radial flux density in the air-gap at one moment(when the voltage is the highest for one phase) (RL)

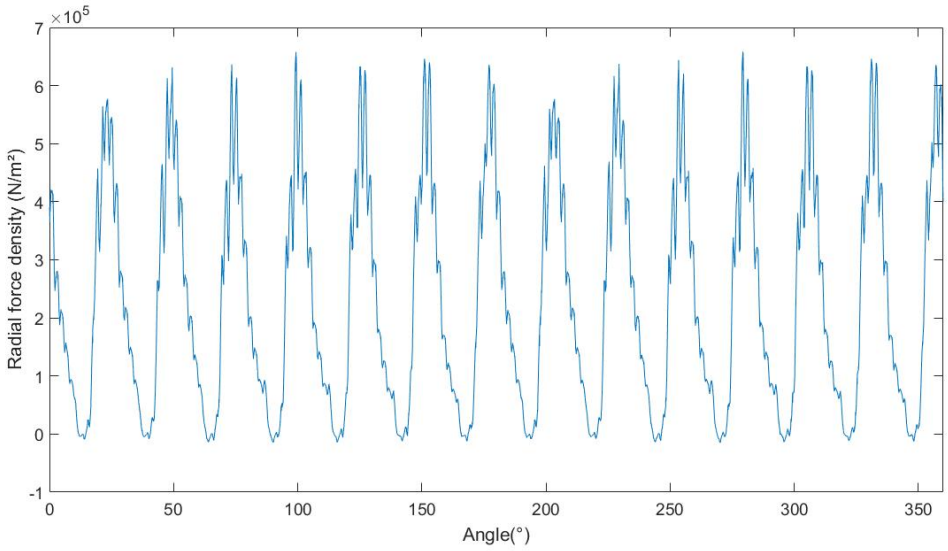

(a) Machine 1

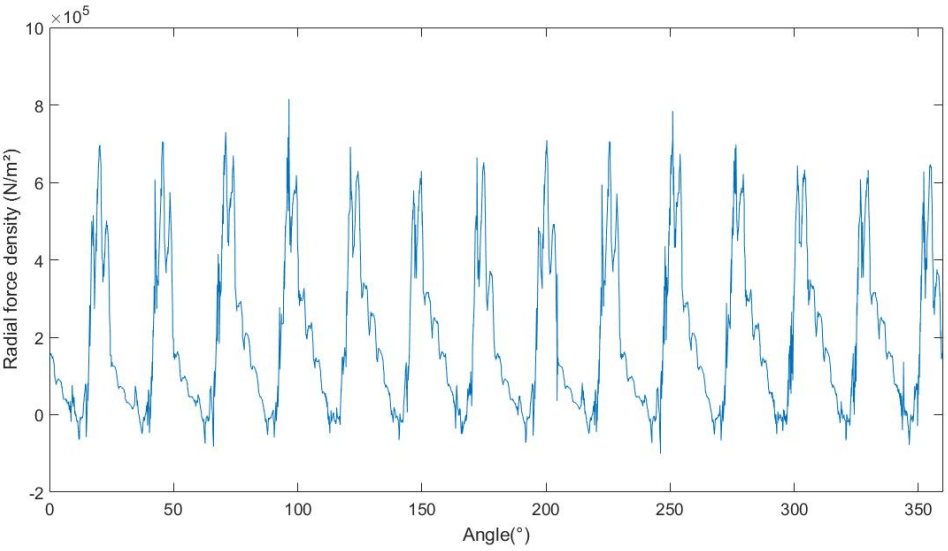

(b) Machine 2

Figure 24: Distribution of the radial force density at one moment(when the voltage is the highest for one phase) (RL)

The harmonic of lowest order can be clearly observed Figures 23a, 23b, 24a and 24b, especially in the force density distribution. The harmonic contents allow to notice that the relative amplitude of the sub-harmonic compared to the main harmonic

is higher in the second machine. The harmonic of order 2 is 10% of the amplitude of the main harmonic for the second machine, whereas it only is 3.8% of it in the first machine Figure 26a and 26b. The same observation can be made with the radial flux density distribution Figure 25a and 25b, the sub-harmonic being 1.627% of the main harmonic amplitude in the second machine and 0.7% in the first machine. The sub-harmonic already exists in the radial flux density distribution, but most of the amplitude of the harmonic of lowest order comes from the interaction between the poles and the slots[12]. This statement can be confirmed by observing how the amplitude of this harmonic increases when the amplitude of the slot harmonic is higher. The amplitude of the sub-harmonic in the flux density distribution was already higher in the second machine, but this difference increases in the radial force density distribution. It is explained by how high is the slot harmonic of the second machine compared to the first one. Because the harmonic of lowest order is mainly caused by the interaction between slots and poles, having a higher amplitude of slot harmonic is susceptible to increase the amplitude of the harmonic of order 2.

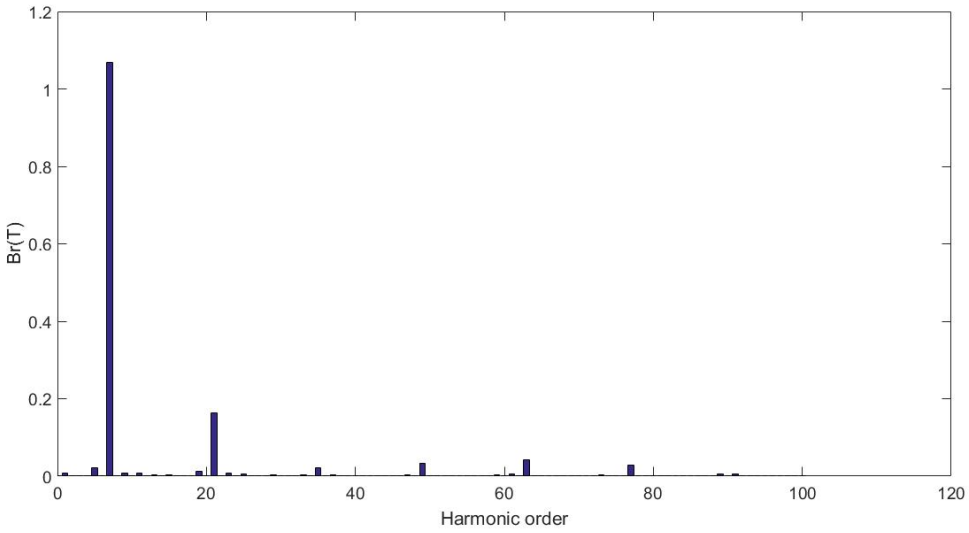

(a) Machine 1

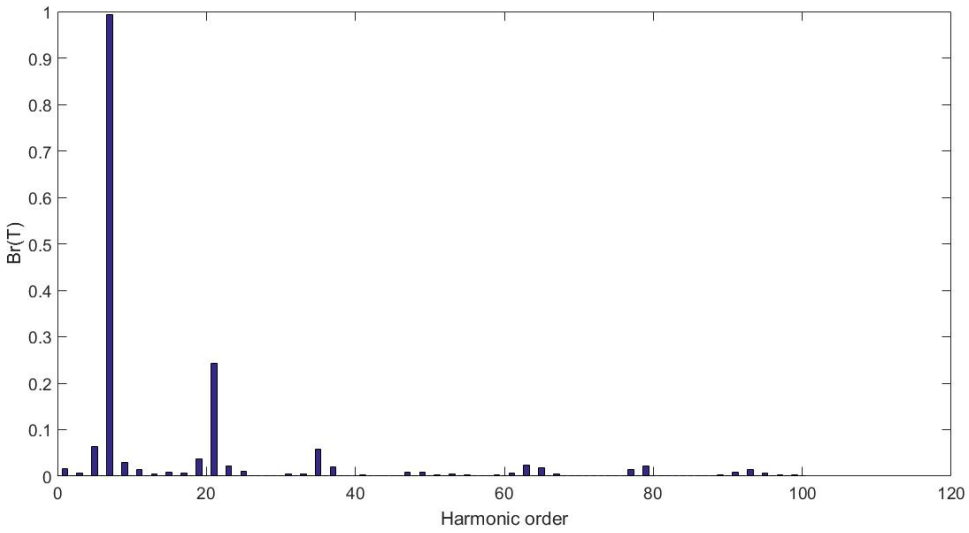

(b) Machine 2

Figure 25: Harmonic content of the radial flux density in the air-gap at one moment(when the voltage is the highest for one phase) (RL)

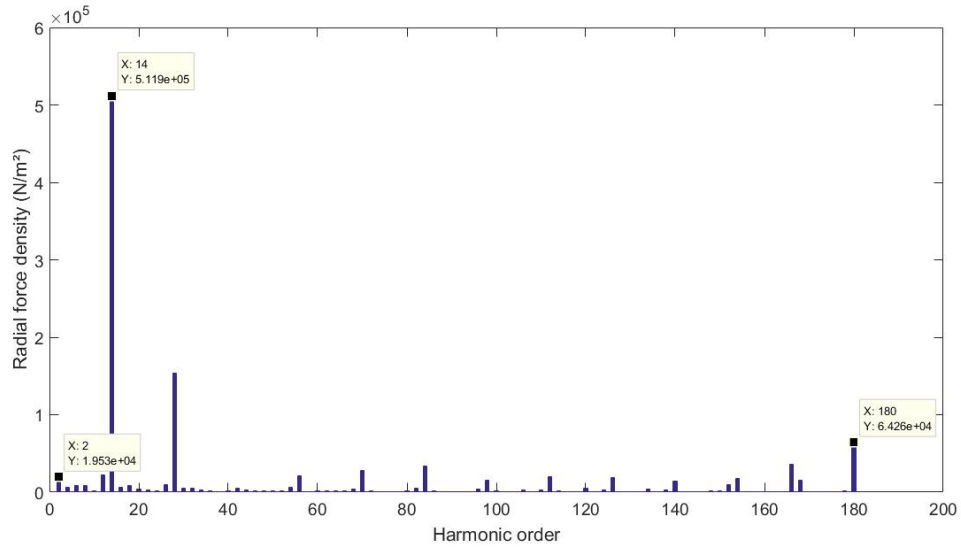

(a) Machine 1

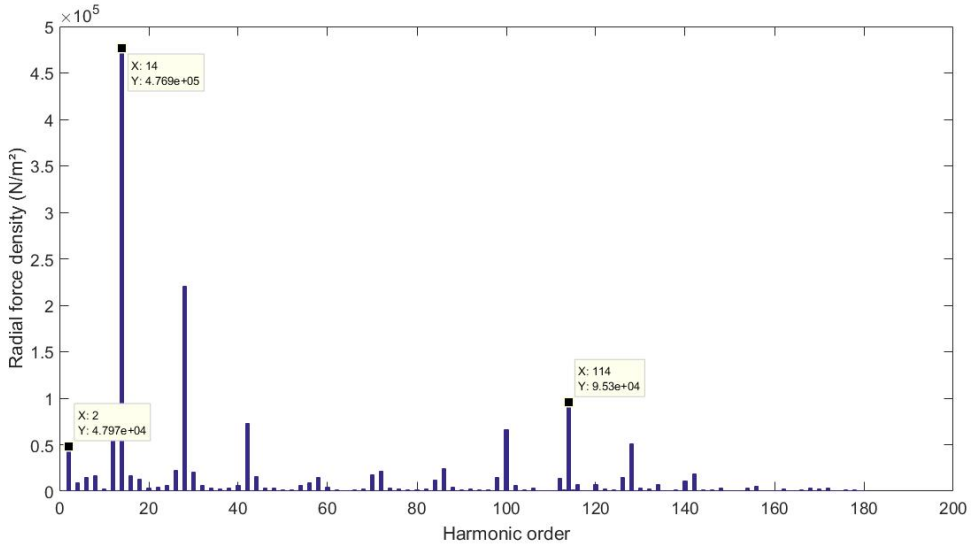

(b) Machine 2

Figure 26: Harmonic content of the radial force density at one moment(when the voltage is the highest for one phase) (RL)

The same conclusions can be made with the results from the simulations with a resistive and a capacitive load shown Figure 27, 28, and 29, also the inductive load makes the differences clearer, thus it will be the only load used for discussions.

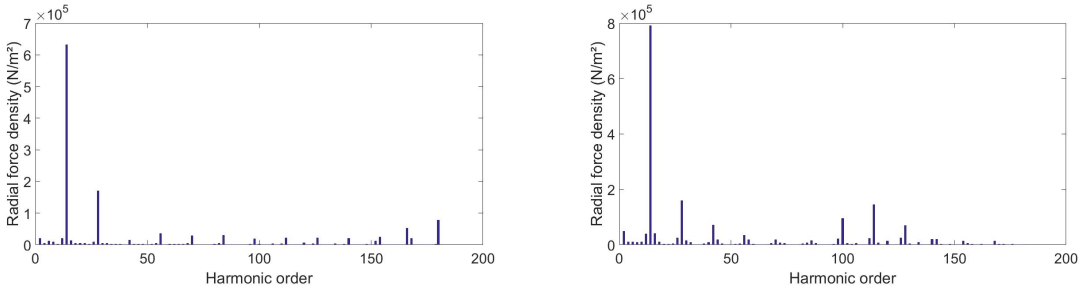

(a) Machine 1 (b) Machine 2

Figure 27: Harmonic content of the radial force density at one moment(when the voltage is the highest for one phase) (R)

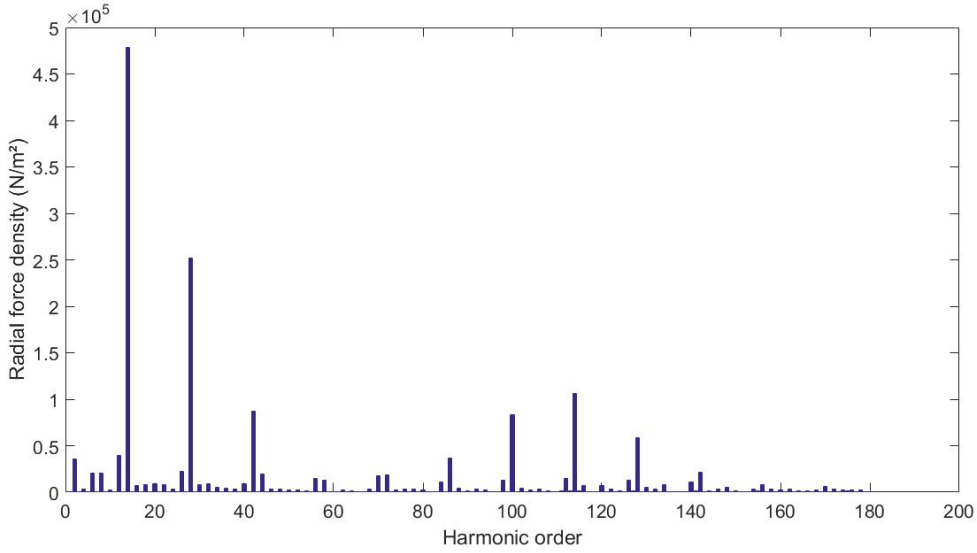

Figure 28: Harmonic content of the radial force density at one moment(when the voltage is the highest for one phase on Machine 2) (R+Diode rectifier)

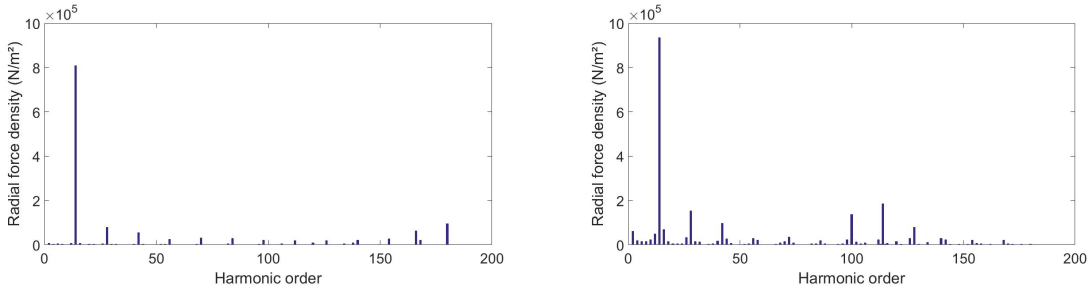

(a) Machine 1 (b) Machine 2

Figure 29: Harmonic content of the radial force density at one moment(when the voltage is the highest for one phase) (RC)

4.3 Zeroth mode of vibration

The last result that should be discussed on those machines is the influence their design had on the zeroth mode of vibration. The amplitude of this mode of vibration is small on both machines, even negligible for the first machine with no load. However, the second machine has small but non negligible zeroth mode amplitude Figure 30, which allows to suppose the effect of the slots width on it. The mean value of the radial force density with the inductive load on the first machine is visible as shown Figure 31. It is still too small to have any repercussion on the stator but it is interesting to compare it with the one of the second machine.

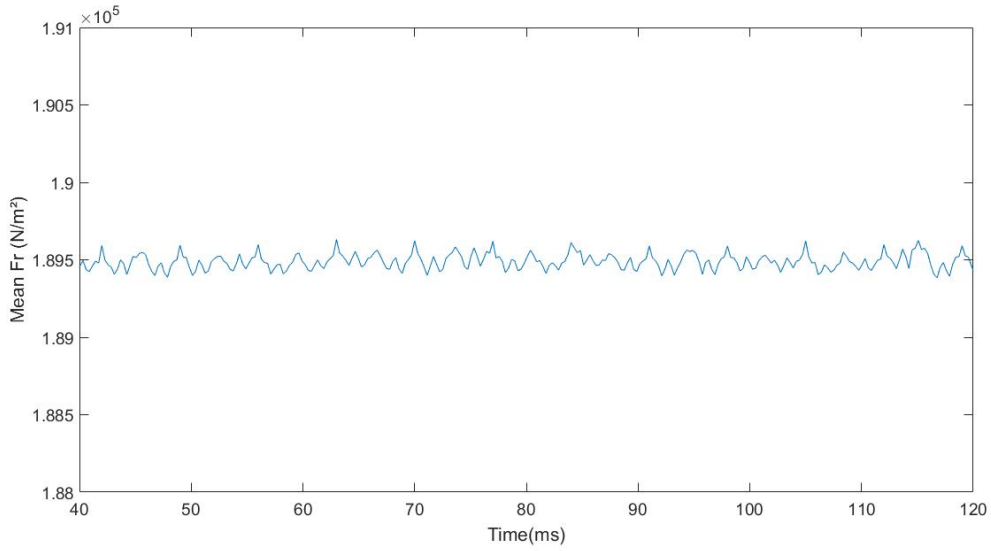

Figure 30: Mean value of the radial force density for a simulation time of 140ms(no load) Machine 2

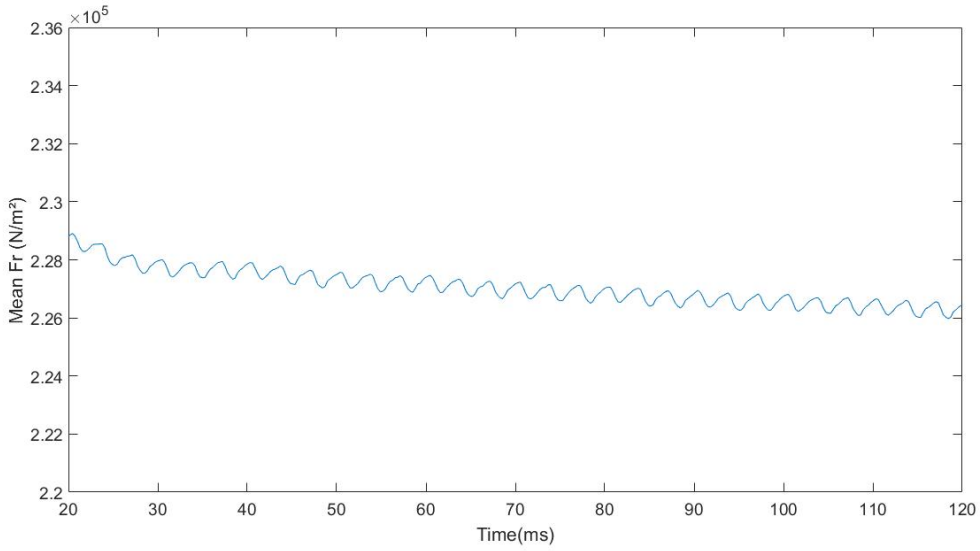

Figure 31: Mean value of the radial force density for a simulation time of 140ms(RL) Machine 1

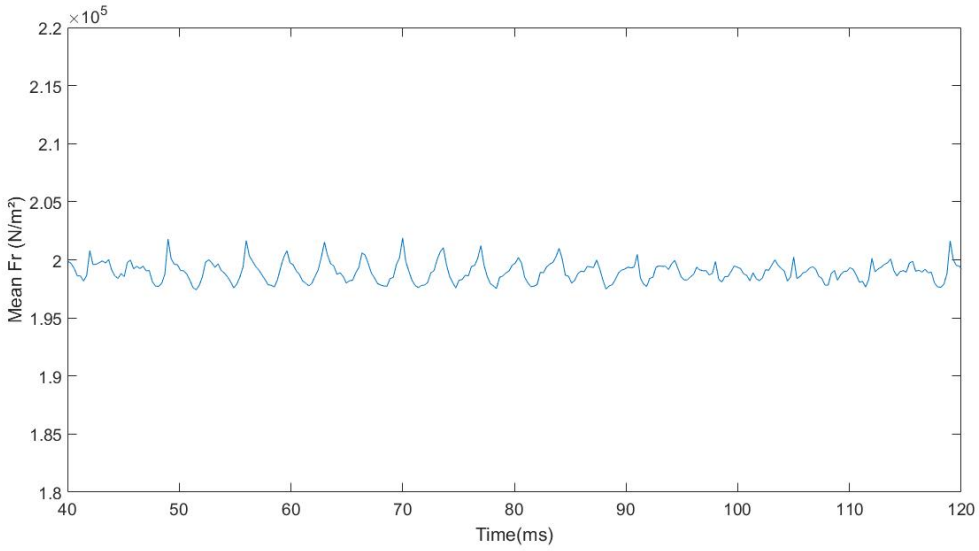

Figure 32: Mean value of the radial force density for a simulation time of 140ms(RL) Machine 2

For the first machine, the amplitude of the oscillation Figure 31 is 1.2% of the average value of the mean radial force, which is much smaller than for the second machine. Indeed, the amplitude of this oscillation Figure 32 is 3.6% of the average value of the mean radial force in the machine 2. These results show that the slot width also has an influence on the amplitude of the zeroth mode of vibration.

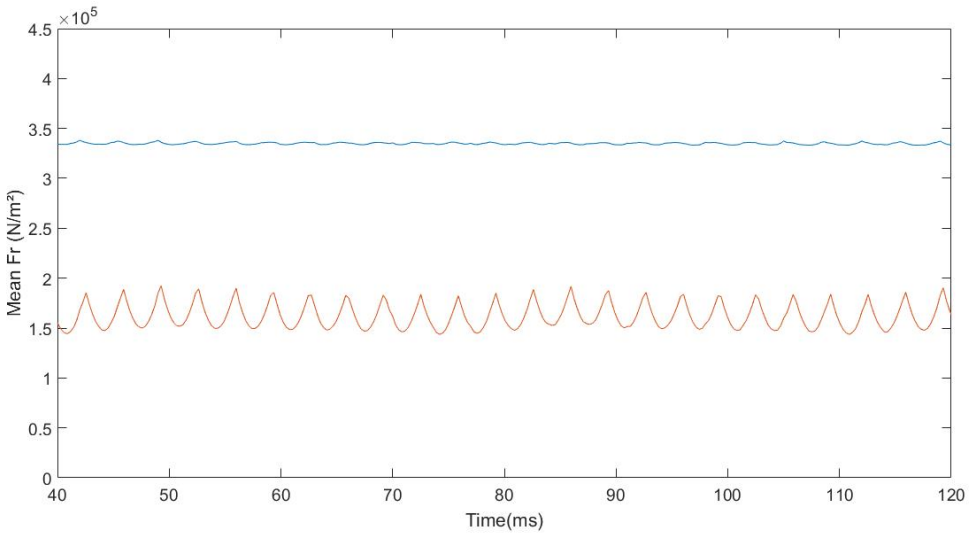

Figure 33: Mean value of the radial force density in machine 2 with and without a diode rectifier
Blue: Without diode rectifier
Red: With diode rectifier

The diode rectifier seems the increase significantly the amplitude of the zeroth mode of vibration. Figure 33 compares it with a three phase resistive load. The diode rectifier makes the amplitude of this mode 12 times higher than the resistive load. However, the amplitude of the zeroth mode from the simulation with an inductive load is about 25% smaller than the pure resistive load amplitude. The diodes increase this amplitude by adding harmonics to the load while an inductive load decreases it by reducing the harmonic content.

Conclusion

In this project, the radial flux density in the air-gap of two machines has been evaluated with a finite element analysis software for a case with an inductive load and a case without any load. Afterwards, the radial force density has been calculated with Matlab and so was the mean value of the radial force density over time. It has been shown that the radial flux density had a sub-harmonic, but the amplitude of it is small, even negligible in the no load case. This shows that the load increases the amplitude of the sub-harmonic, but it also means that the radial flux density is not the main source of harmonic of low order. The analysis of the radial force density spectrum showed how high is the amplitude of the second harmonic relatively to the main harmonic, compared with the results found with the radial flux density. Having two different machines allowed to notice that when the slot harmonic has a higher amplitude, so does the harmonic of lowest order. This suggests that the second harmonic amplitude of the radial force density mainly comes from the interaction between poles and slots harmonics. Also this higher slot harmonic amplitude was due to wider stator slots. Therefore, as a smaller number of slots per pole implies wider slots, the smaller Q the higher the amplitude of the slots harmonic, and so the amplitude of the second harmonic. The zeroth mode of vibration has been investigated as well and it has been shown that even being small in both machines, this mode was more significant in the machine having wider stator slots, and also tends to be more important when the load increases the harmonic content because of elements such as a diode rectifier. It is concluded that a higher slot width increases the the amplitude of the slot harmonic, harmonic of lowest order, and zeroth mode of vibration, which could lead to stator vibration, depending on the material stiffness and stator thickness.

Future work

Even though the slot width of a stator is chosen for other reasons than the sub-harmonic amplitude, such as the manufacturing costs, it could be interesting to know how the sub-harmonic and the vibration mode evolves depending on the slot width. To do so, Machine 2 should be investigated for different slot widths.

5 References

[1] L. Alberti and N. Bianchi *Theory and design of fractional-slot multilayer winding"*, page n4, September 2011

[2] Rudolf Krall, Johann Krenn, Andreas Schmid, *"Fractional Slot Winding versus Distributed Winding using Winding Function Method"*, Part III. FRACTIONAL WINDING VERSUS DISTRIBUTED WINDING p442

[3] Dr. Duane Hanselman (1994), *"Brushless permanent magnet motor design"*, Chap.5: Design variations, p111-113

[4] Mostafa Valavi, Jean Le Besnerais, Arne Nysveen, *"An inverstigation of Zeroth-Order Radial Magnetic Forces in Low-Speed Surface-Mounted Permanent Magnet Machines"*

[5] Bertrand Cassoret, Jean-Philippe Lecointe, Jean-Franois Brudny, *"Noise and Vibrations"*, Section 9.3.1.1 Flux Density in the Air Gap of Electrical Rotating Machines

[6] Devalan P. *"Vibrations des structures - Systmes discrets et poutres,"*, Techniques de lIngnieur, 2001

[7] Z. Q. Zhu, Z. P. Xia, L. J. Wu, and G. W. Jewell, *Analytical modeling and finite-element computation of radial vibration force in fractional-slot permanent-magnet brushless machines, IEEE Trans. Ind. Appl.*, vol. 46, no. 5, pp. 19081918, Sep./Oct. 2010

[8] Hamid A. Toliyat, Gerald B. Kliman *"Handbook of Electric Motors,"* Mechanican consideration p.552, 2004

[9] Juha Pyrhonen, Tapani Jokinen, Valeria Hrabovcova, *"Design of Rotating Electrical Machines Second edition,"* part 2.12 Fractional slot winding, 2013

[10] Figures from the Finite element analysis software Ansys Maxwell

[11] Mostafa Valavi, Arne Nysveen, Robert Nilssen, *"Effects of Loading and Slot Harmonic on Radial Magnetic Forces in Low-Speed Permanent Magnet Machine with Concentrated Windings"*, June 2015

[12] Mostafa Valavi, Arne Nysveen, Robert Nilssen, *"Slot harmonic effect on magnetic forces and vibration in low-speed permanent magnet machines with concentrated windings,"* IEEE Trans. Ind. Appl., vol. 50, no. 5, pp. 2204-3"13, Sept./Oct. 2014

Appendices

Typical data for SURA® M300-35A

T	W/kg at 50 Hz	VA/kg at 50 Hz	A/m at 50 Hz	W/kg at 100 Hz	W/kg at 200 Hz	W/kg at 400 Hz	W/kg at 1000 Hz	W/kg at 2500 Hz
0,1	0,03	0,07	30,9	0,04	0,09	0,23	1,07	4,45
0,2	0,08	0,17	40,2	0,17	0,40	1,00	4,08	16,1
0,3	0,15	0,30	46,4	0,35	0,85	2,15	8,48	33,6
0,4	0,24	0,45	52,1	0,58	1,41	3,61	14,0	56,9
0,5	0,35	0,62	57,9	0,84	2,06	5,36	20,9	86,6
0,6	0,48	0,82	64,4	1,14	2,81	7,42	29,2	124
0,7	0,61	1,05	72,0	1,46	3,66	9,75	39,0	170
0,8	0,76	1,31	81,1	1,83	4,61	12,4	50,6	227
0,9	0,92	1,63	92,6	2,23	5,65	15,4	64,1	297
1,0	1,10	2,03	108	2,66	6,80	18,8	79,8	382
1,1	1,30	2,55	130	3,16	8,09	22,5	98,0	
1,2	1,54	3,32	168	3,72	9,54	26,8		
1,3	1,82	4,71	250	4,39	11,2	31,6		
1,4	2,20	8,61	510	5,23	13,4	37,7		
1,5	2,62	23,7	1440	6,22	15,7	44,3		
1,6	2,98	64,1	3490					
1,7	3,25	138	6700					
1,8	3,41	255	11300					

Loss at 1.5 T , 50 Hz, W/kg	2,62
Loss at 1.0 T , 50 Hz, W/kg	1,10
Anisotropy of loss, %	10
Magnetic polarization at 50 Hz	
H = 2500 A/m, T	1,55
H = 5000 A/m, T	1,65
H = 10000 A/m, T	1,78
Coercivity (DC), A/m	45
Relative permeability at 1.5 T	830
Resistivity, μΩcm	50
Yield strength, N/mm²	370
Tensile strength, N/mm²	490
Young's modulus, RD, N/mm²	185 000
Young's modulus, TD, N/mm²	200 000
Hardness HV5 (VPN)	185

RD represents the rolling direction
TD represents the transverse direction
Values for yield strength (0.2 % proof strength)
and tensile strength are given for the rolling direction
Values for the transverse direction are approximately 5% higher

cogent
Surahammars Bruks AB

June 2008

Appendix 2: Dimensions of a pole and a slot Machine 1

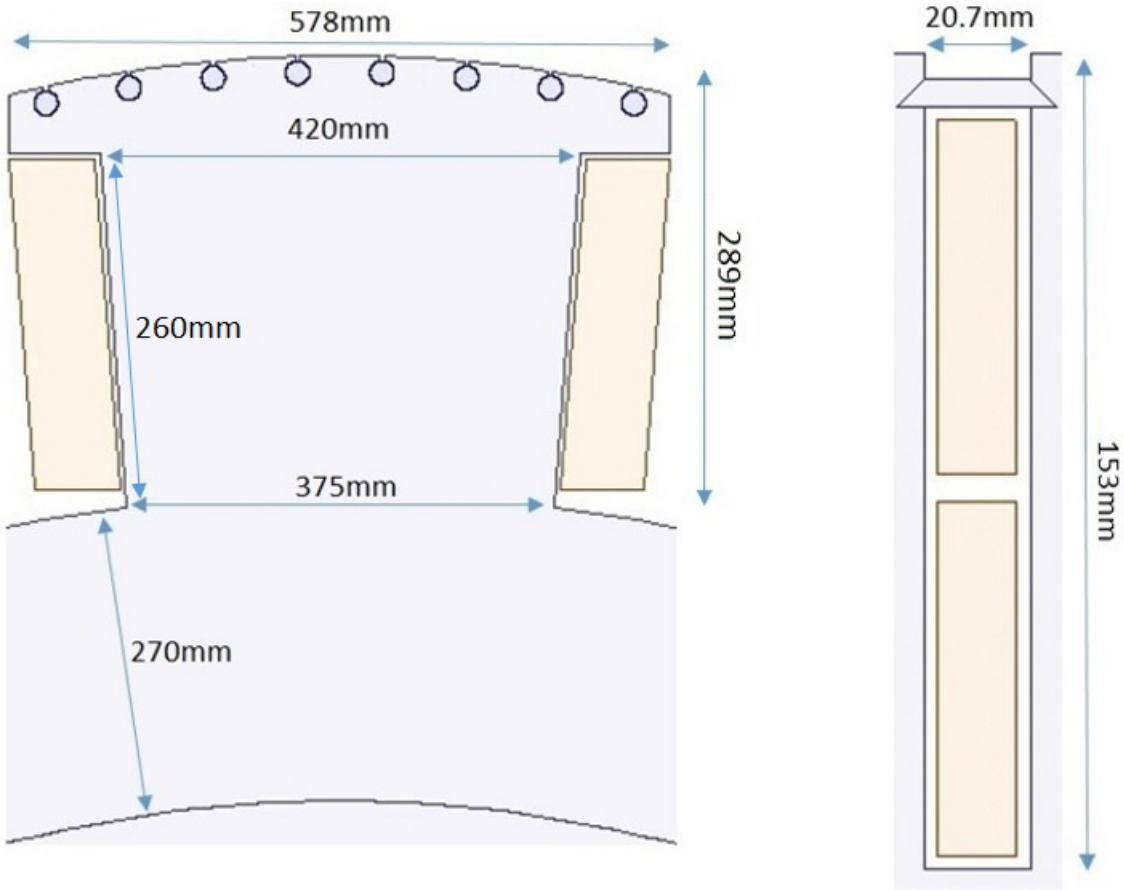

Stator outer diameter	4575mm
Stator inner diameter	3700mm
Rotor diameter	3646mm
Damper bars diameter	21mm
Minimum space between steel and a conductor	2.5mm
Gross iron length	1800mm
Coil pitch	Full pitch